nature nanotechnology

LETTERS

PUBLISHED ONLINE: 2 MARCH 2014 | DOI: 10.1038/NNANO.2014.24

Three-dimensional manipulation with scanning near-field optical nanotweezers

J. Berthelot[1], S. S. Aćimović[1], M. L. Juan[2,3], M. P. Kreuzer[1], J. Renger[1] and R. Quidant[1,4]*

Recent advances in nanotechnologies have prompted the need for tools to accurately and non-invasively manipulate individual nano-objects[1]. Among the possible strategies, optical forces have been predicted to provide researchers with nano-optical tweezers capable of trapping a specimen and moving it in three dimensions[2–4]. In practice, however, the combination of weak optical forces and photothermal issues has thus far prevented their experimental realization. Here, we demonstrate the first three-dimensional optical manipulation of single 50 nm dielectric objects with near-field nanotweezers. The nano-optical trap is built by engineering a bowtie plasmonic aperture at the extremity of a tapered metal-coated optical fibre. Both the trapping operation and monitoring are performed through the optical fibre, making these nanotweezers totally autonomous and free of bulky optical elements. The achieved trapping performances allow for the trapped specimen to be moved over tens of micrometres over a period of several minutes with very low in-trap intensities. This non-invasive approach is foreseen to open new horizons in nanosciences by offering an unprecedented level of control of nanosized objects, including heat-sensitive biospecimens.

Building knowledge within the physical, chemical and biological sciences often requires fractionating complex and macroscopic mechanisms into simpler elementary ones on the nanometre scale. With this aim, researchers have put a great deal of effort into developing techniques for monitoring as well as controllably and non-invasively manipulating elementary units of matter down to the single atom/molecule level. Among these techniques, scanning probe microscopy has played a key role. Originally developed for imaging purposes, scanning tunnelling microscopy became a powerful way to manipulate individual atoms adsorbed at a surface[5]. Slightly later, the atomic force microscope followed a similar route and proved useful in picking up and moving slightly larger amounts of matter, typically with dimensions in the range of tens of nanometres, such as nanocrystals, nanoparticles or carbon nanotubes[6,7]. Interestingly, the optical version of scanning probe microscopy—near-field scanning optical microscopy (NSOM)[8,9]—was originally foreseen to also have nanomanipulation capability. In the 1990s, several theoretical studies predicted that the strong optical concentration produced at the tip of a sharply elongated metallic probe should create optical forces strong enough to stably trap dielectric objects with dimensions as small as a few nanometres[2–4,10–12]. Despite these predictions, this has never been reported experimentally, and has largely been prevented by photothermal effects[9] (L. Novotny, personal communication). Although this configuration offers strong optical gradients, the required level of local field intensity within the trap (larger than 1×10^{12} W m^{-2}), when accounting for the large intensity enhancement at the tip (for example, 3,000; ref. 2), is liable to damage either the specimen being trapped[13] or the tip itself[14–17]. When operating in liquid, absorption within the metal is also responsible for heat-induced fluid dynamics[18] or bubble formation[19], which may further jeopardize trapping. Here, we report on the first realization of optical trapping and manipulation of an individual nano-object at the extremity of an NSOM probe. Our nano-optical tweezers are formed at the extremity of a metal-coated tapered optical fibre patterned with a bowtie nano-aperture (BNA). We demonstrate stable optical trapping and accurate three-dimensional manipulation of a 50 nm polystyrene bead in water with local intensities within the trap as small as 1×10^{9} W m^{-2}. Such a level of intensity sits well below what would be required for conventional optical tweezers (typically from 1×10^{11} to 1×10^{12} W m^{-2}) and is compatible with heat-sensitive objects such as biospecimens.

Our present work capitalizes on the latest advances in near-field optical trapping[20–22] based on the so-called self-induced back-action (SIBA) mechanism, which dramatically relaxes the requirements on the local optical intensity and thus minimizes photothermal issues[23]. In SIBA trapping, the resonant optical nanostructure is designed such that its optical properties (resonance spectrum, local field distribution and intensity) significantly depend on the presence of the specimen. For a trapping laser slightly redshifted with respect to the central resonance wavelength of the nanostructure, the trap becomes stiffer when the specimen tends to escape as the result of the induced resonance shift. In other words, the trapped specimen plays an active role in the trapping mechanism in such a way that the required average local field intensity is weaker by orders of magnitude when compared with conventional trapping. Interestingly, the trap reconfiguration does not require any active monitoring of the specimen as it is automatically synchronized with its dynamics[24–26].

In practice, implementing SIBA trapping at the extremity of a tapered optical fibre first requires identifying a geometry of the SIBA trap that enables extended trapping times under low laser intensity, to prevent any photothermal damage at the fibre extremity. The typical damage threshold for such probes lies around 1×10^{10} W m^{-2} at the tip apex[17]. To remain below this threshold, we focused our attention on the so-called BNA design[27–29]. This geometry combines high collection cross-section and transmission with strong mode confinement under transversal polarization, making it a very good candidate for SIBA trapping. BNA supports two types of resonance: a Fabry–Pérot-like resonance that mainly depends on the film thickness, as well as two plasmonic resonances that depend on the geometry of the aperture[28]. Extensive three-dimensional numerical simulations based on COMSOL were performed to identify the most suitable design to achieve SIBA trapping at 1,064 nm on 100-nm-thick gold film covered with water. Parameters were chosen such that the transverse plasmonic mode (confined within the gap region) was slightly blue-detuned with respect to the trapping

[1]ICFO – Institut de Ciencies Fotoniques, Mediterranean Technology Park, 08860 Castelldefels (Barcelona), Spain, [2]Department of Physics & Astronomy, Macquarie University, Sydney, New South Wales 2109, Australia, [3]ARC Centre for Engineered Quantum Systems, Macquarie University, Sydney, New South Wales 2109, Australia, [4]ICREA – Institució Catalana de Recerca i Estudis Avançats, 08010 Barcelona, Spain. *e-mail: romain.quidant@icfo.es

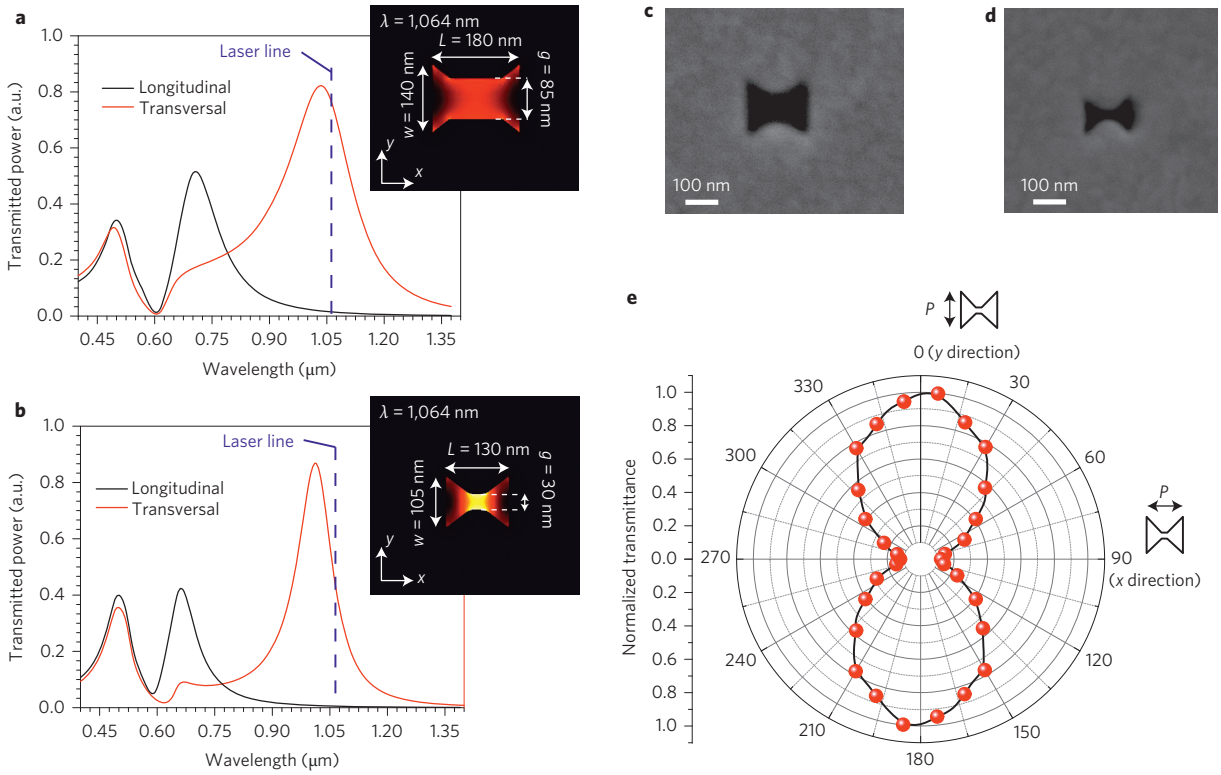

Figure 1 | Optical properties of BNAs. a–d, Calculated transmission spectra and near-field intensity maps (**a**,**b**) at 1,064 nm under transverse incident polarization for the two fabricated BNAs presented in the SEM images (**c**,**d**, respectively). **e**, Evolution of the experimental transmission at 1,064 nm as a function of incident polarization, *P*, for a 30 nm gap BNA.

wavelength. This condition was fulfilled for gap sizes between 30 nm and 85 nm by adjusting both the length and width of the antenna. Based on these simulations, BNAs were first fabricated in a planar geometry to evaluate and optimize their trapping performance. Figure 1c,d presents scanning electron microscopy (SEM) images of two fabricated apertures, with 85 nm and 30 nm gaps, respectively. The transmission spectra and near-field maps at 1,064 nm displayed in Fig. 1a,b were calculated from the experimental geometrical parameters extracted from Fig. 1c,d. As expected, the transverse mode confinement increases for decreasing gap sizes. In agreement with earlier studies, the enhancement of the local electric field intensity at the centre of the gap ranges from below 100 for the 30 nm gap to below 10 for the 85 nm gap[30]. To probe the transverse mode of the fabricated BNA, we also measured the evolution of the transmission through the aperture at 1,064 nm as a function of the incident polarization. In good agreement with the simulations, the polar transmission plot of a 30 nm gap BNA (Fig. 1e) features a maximum when the incident electric field aligns across the gap (*y* axis).

Figure 2 illustrates the trapping performance of a BNA with a 30 nm gap. The aperture was exposed to a diluted aqueous solution (0.05% wt/vol) of 20 nm fluorescent polystyrene beads (absorption at 532 nm/emission at 612 nm) containing a 1% concentration of SDS solution to prevent aggregation. Figure 2a provides a schematic of the experimental configuration. The 1,064 nm trapping laser was linearly polarized along the *y* axis before being slightly focused (from the water side) onto the BNA with a ×40 objective lens (0.65 NA), producing an illumination spot of ~2 μm. A 532 nm laser was added to the same optical path to simultaneously excite the bead fluorescence. The transmission through the BNA at 1,064 nm and the fluorescence from the bead were monitored over time by two independent photodetectors (see Methods). A typical portion of the experimental time traces, demonstrating optical trapping of a single 20 nm bead for an irradiance of 1.27×10^9 W m^{-2}, is presented in Fig. 2b. Trapping was monitored by the increase of the transmission signal resulting from the local increment of refractive index induced by the presence of the particle[23–25]. Statistical analysis of the data enabled the identification of two transmission levels corresponding to an empty trap and trapping of a single bead. This interpretation was further confirmed by the fluorescence time trace, which displays an increase exactly coinciding with the increased level of transmission. Trapping times longer than 30 min were achieved under these illumination conditions. We also systematically checked that the trapped nanoparticle did not stick to the antenna and was released when switching off the trapping laser (Supplementary Fig. 1). To test the robustness of SIBA trapping with the BNA geometry, we also performed additional experiments using larger gaps of 85 nm. Despite the weaker confinement of the mode (translating into a weaker effect of the trapped specimen on the BNA resonance), both 50 nm and 20 nm polystyrene beads were successfully trapped over several minutes using incident powers between 2 and 5 mW (0.63×10^9 W m^{-2} and 1.59×10^9 W m^{-2}), respectively.

At this stage, optimized in-plane BNA trapping was implemented at the extremity of a scanning tapered metallized optical fibre to achieve nano-optical tweezers capable of manipulating the trapped specimen in three dimensions. The fabrication process used to prepare the tapered fibres was adapted from ref. 17. Briefly, a single-mode optical fibre was tapered by laser pulling and coated with 200 nm aluminium to prevent light leakage through the sides of the cone. Focused ion beam (FIB) milling was used to cut the tip extremity to obtain a flat facet, which was subsequently metallized with 100 nm of gold. Finally, the BNA was milled by FIB at the centre of the 1-μm-diameter gold platform. An example of a fabricated tweezers is shown in the SEM image in Fig. 3a. It is worth mentioning that, with the FIB we used, fabrication of the 30-nm-gap BNAs required exposure

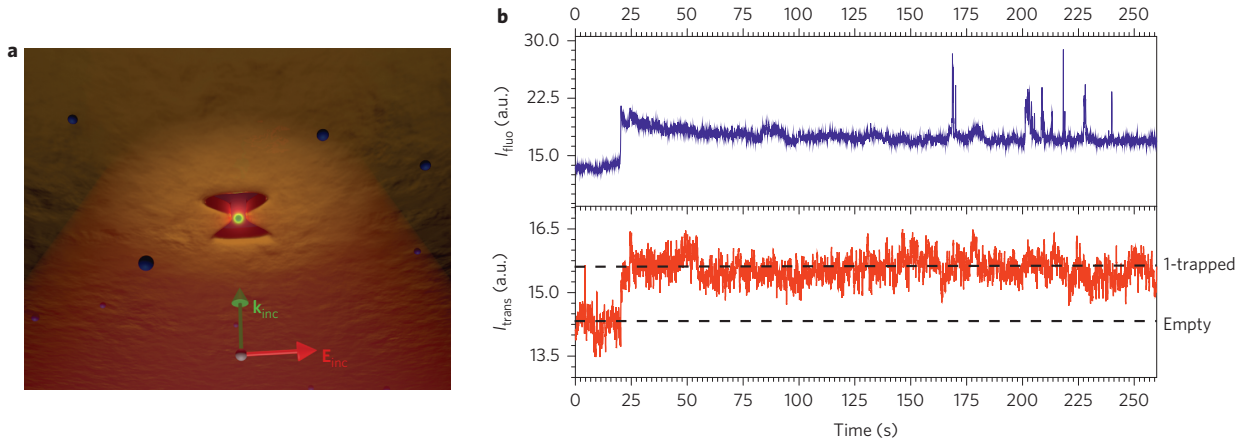

Figure 2 | SIBA trapping of a single 20 nm polystyrene bead in a planar geometry. a, Schematic of experimental configuration. A 30-nm-gap BNA is illuminated from the water side with a 1,064 nm laser beam, linearly polarized along the *y* axis, and slightly focused with a ×40 (0.65 NA) objective lens. **b**, Experimental time traces showing transmission through the BNA at 1,064 nm (red curve) and fluorescence from the trapped bead (blue curve). The increase in both transmission and fluorescence corresponds to the trapping of a single 20 nm polystyrene bead.

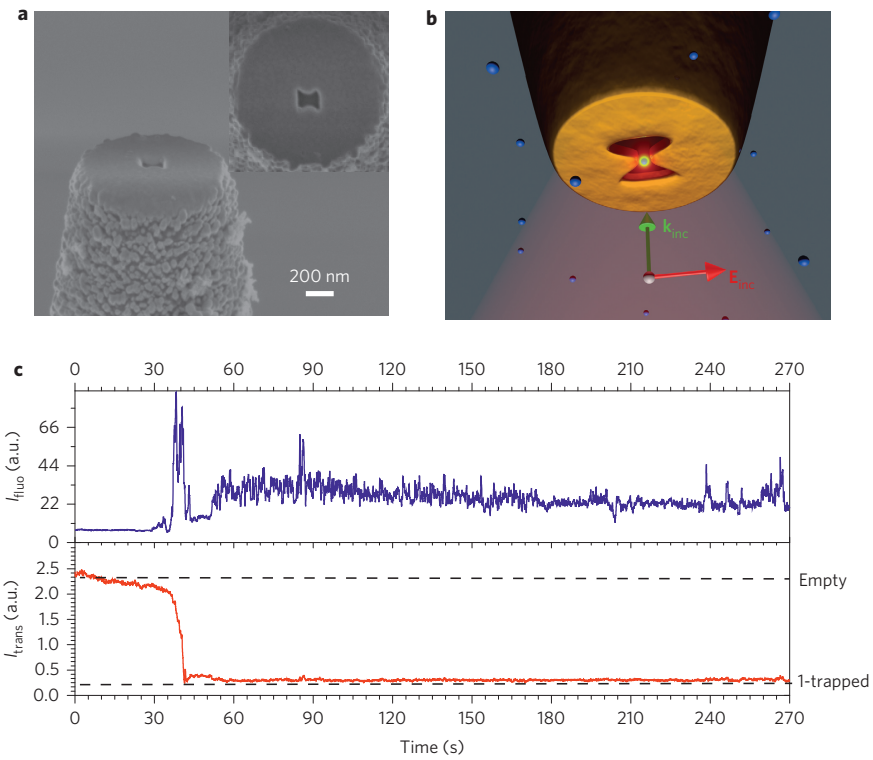

Figure 3 | SIBA trapping at the extremity of a patterned tapered fibre under external illumination. a, SEM image of an 85-nm-gap BNA patterned at the extremity of a tapered optical fibre. **b**, Schematic of the experimental configuration: the antenna is illuminated from the water side with a 1,064 nm laser beam focused through a ×40 (0.65 NA) objective. The incident polarization is aligned along the BNA gap to excite its transverse mode. **c**, Portion of the time traces of the 1,064 nm signal detected by the fibre (red) and the fluorescence from the bead (blue) detected by the objective lens. A 50 nm polystyrene bead enters the aperture area around $t = 35$ s and is stably trapped after $t = 40$ s.

parameters that were not compatible with fully preserving the integrity of the fibre output facet. For this reason, in the following, we limit ourselves to gaps of 85 nm. For the trapping experiments, the fabricated fibres were mounted on a three-dimensional piezoelectric scanner and introduced into a modified fluidic chamber (see Methods) containing a solution of 50 nm polystyrene beads (same parameters as in the in-plane experiments). We tested two trapping schemes based on different illumination conditions; either through an objective lens or through the fibre itself.

In the first configuration, schematically presented in Fig. 3b, the 1,064 nm laser was focused through the ×40 objective (0.65 NA) and centred on the BNA. The transmitted light was collected through the fibre and sent to a silicon photodetector. The fluorescence from the bead was collected back through the same objective lens before being focused on an avalanche photodiode using a confocal detection. Figure 3c presents a portion of typical time traces, demonstrating the trapping of a single 50 nm bead using an incident power of 4 mW (1.27×10^9 W m^{-2}). In this

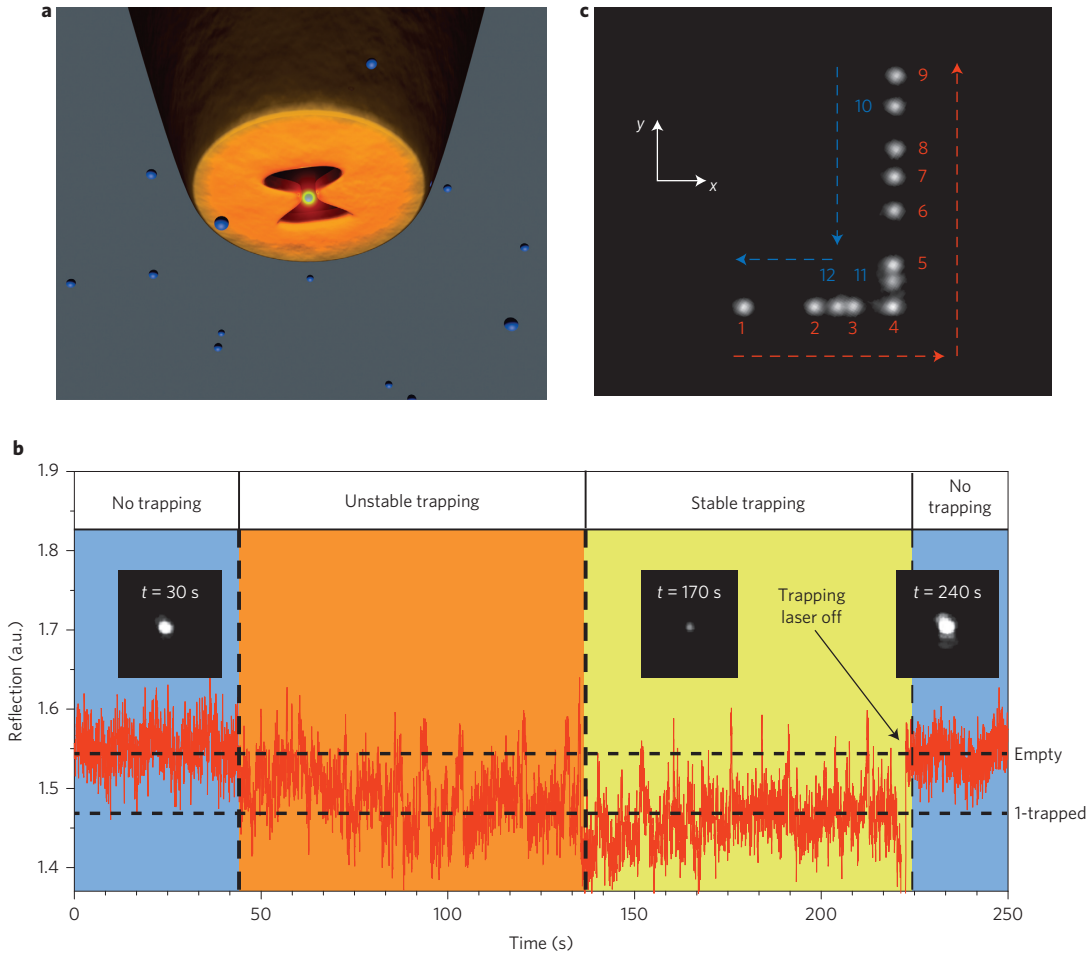

Figure 4 | Three-dimensional manipulation of a single 50 nm polystyrene bead. a, Schematic of experimental configuration. The 1,064 nm trapping laser is directly coupled into the fibre to excite the transverse mode of the BNA. **b**, Experimental time trace of the reflected 1,064 nm signal showing trapping of a single 50 nm polystyrene bead. Insets: Optical images of the fibre transmission spot at different times. **c**, Composite image reproducing the displacement of the trapped object. This displacement takes place during the time period $t = 180$–210 s of time trace **b**. Numbers 1–12 represent the successive steps of the tip movement. See also Supplementary Movie.

configuration, unlike what was observed in the planar sample, the trapping event is associated with a decrease in the transmitted signal. This decrease is attributed to the detection through the fibre. Because of its subwavelength size, the nanobead scatters light over a wide range of **k**-vectors, thus decreasing the amount of light coupled into the fibre mode. This interpretation is consistent with the simultaneous increase in the fluorescence signal, confirming the presence of the nanobead within the BNA. As for the in-plane configuration, we verified that the particle was released when switching off the trapping laser (Supplementary Fig. 2). Although stable trapping was achieved for more than 3 min, this configuration has some issues. First, the trap position is fixed and does not take advantage of the tip mobility. Second, because the tapered fibre and the collection objective are physically independent, vibrations and small drifts in their relative position produce additional noise, making monitoring and analysis of the trapping events more difficult.

To overcome these issues, we switched to the second configuration where both illumination and collection are performed through the fibre. For this purpose we implemented a (90/10) fibre coupler combined with a polarization-maintaining (PM) fibre designed for 1,064 nm. Polarization of the incoming 1,064 nm laser (10% arm) was controlled at the entrance of the PM fibre and set to maximize the transmission through the BNA. The 1,064 nm light reflected by the tapered end face of the fibre was then collected by the 90% arm and focused on a silicon photodetector. A schematic of the experimental configuration is provided in Fig. 4a. With this configuration, both excitation and detection can be made using only the fibre. Additionally, the transmission collected by a ×40 objective (0.65 NA) was imaged on a charge-coupled device (CCD) camera. A typical time trace of the reflected signal through the fibre is plotted in Fig. 4b. To estimate the incident intensity reaching the BNA plane, power measurements were systematically performed on aluminized tapered fibres before deposition of the gold layer. Powers ranging from 350 to 675 μW, depending on the taper angle, were measured at the output of the fibre end facet. The corresponding local intensities ranging from 4×10^9 W m^{-2} to 8×10^9 W m^{-2} (accounting for the tenfold theoretical intensity enhancement within the antenna gap) sit below the fibre damage threshold[17]. Similar to the previous trapping experiment, we identify in Fig. 4b two different levels in the reflected 1,064 nm signal, corresponding to the empty trap (higher level) and trapping of a single nanobead (lower level) (Supplementary Fig. 3). Trapping also corresponds to a decrease in the intensity of the transmitted signal recorded by the CCD camera. A closer look at the time trace of Fig. 4b enables us to distinguish three successive regimes: no trapping (blue area), unstable trapping (orange area) and stable trapping (yellow area). During the unstable trapping regime

(40 s $< t <$ 135 s), the nanobead moves within the BNA without reaching the equilibrium position in the gap region, leading to large fluctuations in both the reflected and transmitted signals. As this behaviour was not observed in the previous configuration, this suggests that the illumination through the objective helps to push the particle towards the equilibrium position. Around $t = 140$ s, both signals become more steady, with the beginning of a stable trapping regime. Once the stable trapping regime was reached, the fibre was raster-scanned in all three spatial directions (see Supplementary Movie). The scan trajectory is shown in Fig. 4c, in which we have superimposed different CCD images from different time instances. The displacement of the tip was ~15 μm in the plane (x–y) and ~5 μm in the z direction. Finally, we verified that the trapped nanobead did not stick to the BNA and could be released by blocking the trapping beam ($t = 215$ s).

In conclusion, we have developed the first nano-optical tweezers capable of three-dimensionally manipulating (with nanometre accuracy) sub-100-nm dielectric objects over large ranges. We envision this approach could open new opportunities in various fields of science. In the context of biology it may enable non-invasive manipulation of individual nano-units such as viruses or large proteins[31]. It may also benefit the field of materials science, with the possibility of isolating, manipulating and controllably arranging solid-state nano-objects such as nanocrystals.

Methods

Microfluidic chamber for fibre trapping. The fluidic chamber used for fibre trapping was made of polydimethylsiloxane (PDMS) and a curing agent (5:1 by volume). With this mixture we obtained a PDMS piece measuring 20 mm × 20 mm × 5 mm. The chamber volume was made by removing the inner part of this piece. A thin membrane made with a solution of PDMS/curing agent (20:1 by volume) was fixed on top to prevent liquid evaporation. A hole (2 mm in diameter) was created in the centre of the membrane, allowing the introduction of the structured fibre. The complete PDMS piece was chemically bonded (12 h at 80 °C in the oven) to a 170-μm-thick glass substrate. The chamber was then completely filled with the solution of nanobeads via an inlet.

Optical set-up. We used a homemade inverted microscope. The trapping laser was a continuous-wave 1,064 nm Nd-YAG laser, the beam of which was extended and collimated to an 8-mm-diameter beam before being focused on the sample plane with a dry ×40 microscope objective (0.65 NA). A visible diode laser at 532 nm was focused on the sample at the same position as the trapping laser to excite bead fluorescence, and the same objective was used for fluorescence excitation and collection. The collected fluorescence was separated from the trapping laser beam with a dichroic mirror (reflecting 532 nm and 1,064 nm, and transmitting otherwise) and bandpass filter (580 nm to 640 nm), and then focused onto an avalanche photodiode in a confocal detection mode. The transmission of the trapping laser through the BNA was collected with a ×10 dry objective (0.22 NA) and sent to a photodiode. The polarization of the 1,064 nm laser was controlled by a polarizer and a half-wave plate. The incoming laser power was limited to a maximum of 10 mW in the sample plane. The acquisition signals were obtained using a Labview program at a sampling rate of 1 kHz.

Received 8 November 2013; accepted 20 January 2014; published online 2 March 2014

References

1. Maragò, O. M., Jones, P. H., Gucciardi, P. G., Volpe, G. & Ferrari, A. C. Optical trapping and manipulation of nanostructures. *Nature Nanotech.* **8,** 807–819 (2013).
2. Novotny, L., Bian, R. & Xie, X. Theory of nanometric optical tweezers. *Phys. Rev. Lett.* **79,** 645–648 (1997).
3. Martin, O. J. F. & Girard, C. Controlling and tuning strong optical field gradients at a local probe microscope tip apex. *Appl. Phys. Lett.* **70,** 705–707 (1997).
4. Chaumet, P., Rahmani, A. & Nieto-Vesperinas, M. Optical trapping and manipulation of nano-objects with an apertureless probe. *Phys. Rev. Lett.* **88,** 123601 (2002).
5. Hla, S-W. Scanning tunneling microscopy single atom/molecule manipulation and its application to nanoscience and technology. *J. Vac. Sci. Technol. B* **23,** 1351–1360 (2005).
6. Kim, S., Shafiei, F., Ratchford, D. & Li, X. Controlled AFM manipulation of small nanoparticles and assembly of hybrid nanostructures. *Nanotechnology* **22,** 115301 (2011).
7. Decossas, S. *et al.* Nanomanipulation by atomic force microscopy of carbon nanotubes on a nanostructured surface. *Surf. Sci.* **543,** 57–62 (2003).
8. Betzig, E., Lewis, A., Harootunian, A., Isaacson, M. & Kratschmer, E. Near field scanning optical microscopy (NSOM): development and biophysical applications. *Biophys. J.* **49,** 269–279 (1986).
9. Hecht, B. *et al.* Scanning near-field optical microscopy with aperture probes: fundamentals and applications. *J. Chem. Phys.* **112,** 7761–7774 (2000).
10. H'dhili, F., Bachelot, R., Lerondel, G., Barchiesi, D. & Royer, R. Near-field optics: direct observation of the field enhancement below an apertureless probe using a photosensitive polymer. *Appl. Phys. Lett.* **79,** 4019–4021 (2001).
11. Chaumet, P., Rahmani, A. & Nieto-Vesperinas, M. Photonic force spectroscopy on metallic and absorbing nanoparticles. *Phys. Rev. B* **71,** 045425 (2005).
12. Okamoto, K. & Kawata, S. Radiation force exerted on subwavelength particles near a nanoaperture. *Phys. Rev. Lett.* **83,** 4534–4537 (1999).
13. Ashkin, A., Dziedzic, J., Bjorkholm, J. & Chu, S. Observation of a single-beam gradient-force optical trap for dielectric particles in air. *Opt. Lett.* **22,** 816–818 (1986).
14. Xin, H., Xu, R. & Li, B. Optical trapping, driving, and arrangement of particles using a tapered fibre probe. *Sci. Rep.* **2,** 818 (2012).
15. Liberale, C. *et al.* Miniaturized all-fibre probe for three-dimensional optical trapping and manipulation. *Nature Photon.* **1,** 723–727 (2007).
16. Liu, Z., Guo, C., Yang, J. & Yuan, L. Tapered fiber optical tweezers for microscopic particle trapping: fabrication and application. *Opt. Express* **14,** 12510–12516 (2006).
17. Neumann, L. *et al.* Extraordinary optical transmission brightens near-field fiber probe. *Nano Lett.* **11,** 355–360 (2011).
18. Donner, J., Baffou, G., McCloskey, D. & Quidant, R. Plasmon-assisted optofluidics. *ACS Nano* **5,** 5457–5462 (2011).
19. Fang, Z. *et al.* Evolution of light-induced vapor generation at a liquid-immersed metallic nanoparticle. *Nano Lett.* **13,** 1736–1742 (2013).
20. Righini, M. *et al.* Nano-optical trapping of Rayleigh particles and *Escherichia coli* bacteria with resonant optical antennas. *Nano Lett.* **9,** 3387–3391 (2009).
21. Grigorenko, A. N., Roberts, N. W., Dickinson, M. R. & Zhang, Y. Nanometric optical tweezers based on nanostructured substrates. *Nature Photon.* **2,** 365–370 (2008).
22. Juan, M. L., Righini, M. & Quidant, R. Plasmon nano-optical tweezers. *Nature Photon.* **5,** 349–356 (2011).
23. Juan, M. L., Gordon, R., Pang, Y., Eftekhari, F. & Quidant, R. Self-induced back-action optical trapping of dielectric nanoparticles. *Nature Phys.* **5,** 915–919 (2009).
24. Pang, Y. & Gordon, R. Optical trapping of 12 nm dielectric spheres using double-nanoholes in a gold film. *Nano Lett.* **11,** 3763–3767 (2011).
25. Chen, C. *et al.* Enhanced optical trapping and arrangement of nano-objects in a plasmonic nanocavity. *Nano Lett.* **12,** 125–132 (2012).
26. Descharmes, N., Dharanipathy, U. P., Diao, Z., Tonin, M. & Houdré, R. Observation of backaction and self-induced trapping in a planar hollow photonic crystal cavity. *Phys. Rev. Lett.* **110,** 123601 (2013).
27. Kinzel, E. C. & Xu, X. Extraordinary infrared transmission through a periodic bowtie aperture array. *Opt. Lett.* **35,** 992–994 (2010).
28. Guo, H. *et al.* Optical resonances of bowtie slot antennas and their geometry and material dependence. *Opt. Express* **16,** 7756–7766 (2008).
29. Jin, E. X. & Xu, X. Plasmonic effects in near-field optical transmission enhancement through a single bowtie-shaped aperture. *Appl. Phys. B* **84,** 3–9 (2006).
30. Mivelle, M., van Zanten, T. S., Neumann, L., van Hulst, N. F. & Garcia-Parajo, M. F. Ultrabright bowtie nanoaperture antenna probes studied by single molecule fluorescence. *Nano Lett.* **12,** 5972–5978 (2012).
31. Pang, Y. & Gordon, R. Optical trapping of a single protein. *Nano Lett.* **12,** 402–406 (2012).

Acknowledgements

This work was partially supported by the Spanish Ministry of Sciences (grants FIS2010–14834), the European Community's Seventh Framework Programme (grant ERC-Plasmolight; no. 259196) and Fundació privada CELLEX. The authors thank M. Mivelle and M. García-Parajo for discussions.

Author contributions

J.B., M.L.J. and R.Q. conceived and designed the experiment. J.B. performed the experiments and analysed the data. S.S.A. performed the numerical simulations. All authors discussed the results and wrote the manuscript.

Additional information

Supplementary information is available in the online version of the paper. Reprints and permissions information is available online at www.nature.com/reprints. Correspondence and requests for materials should be addressed to R.Q.

Competing financial interests

The authors declare no competing financial interests.

nature nanotechnology

SUPPLEMENTARY INFORMATION

DOI: 10.1038/NNANO.2014.24

Three-dimensional manipulation with scanning near-field optical nanotweezers

J. Berthelot [1], S. S. Aćimović [1], M. L. Juan [2,3], M. P. Kreuzer [1], J. Renger [1] and R. Quidant [1, 4, ⋆]

[1] ICFO - Institut de Ciencies Fotoniques, Mediterranean Technology Park, 08860 Castelldefels (Barcelona), Spain

[2] *Department of Physics & Astronomy, Macquarie University, Sydney, NSW 2109, Australia*

[3] *ARC Centre for Engineered Quantum Systems, Macquarie University, Sydney, NSW 2109, Australia*

[4] *ICREA – Institució Catalana de Recerca i Estudis Avançats, 08010 Barcelona, Spain*

Trapping vs. adsorption (planar sample)

For each trapping experiment, we verified that the particle does not stick to the antenna and was indeed maintained in the trap by the optical forces. Initially the particle was stably trapped for several hundreds of seconds. In the following step the trapping laser was switched off to release the particle and we then checked that the transmission reverted back to its initial value i.e. before any particle was trapped. Indeed, in case the particle would be sticking to the antenna, no change in the transmission would be noted once the trapping laser had been switched off.

Figure SI1 presents the trapping of a single 20 nm PS bead via both the transmission through the antenna and the associated fluorescence of the bead. The particle is clearly trapped after t=15 s, the trapping laser is then switched off at t=336 s for 25 s. During this time, the fluorescence is still excited and shows important fluctuations. The latter ones have to be attributed to the fact that particles move across the detection volume.

DOI: 10.1038/NNANO.2014.24

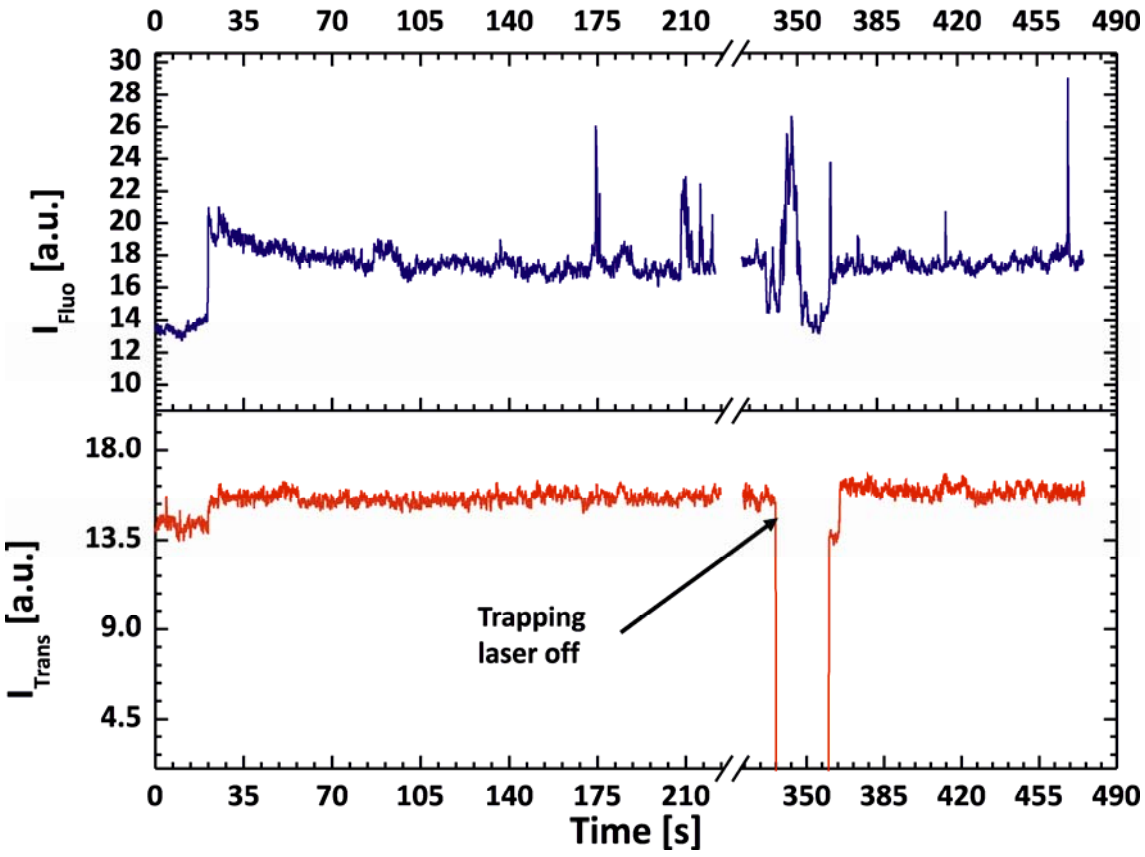

Figure SI1 : Experimental time traces showing trapping and release of a 20 nm PS particle with an in-plane Bowtie nanoaperture: Transmission (in red) and associated fluorescence (in blue). Around t=340 s the trapping laser is switched off while maintaining the green excitation laser on. The trapping laser is switched back on at t=360 s whereby a new particle gets trapped at t=375 s.

At around t=360 s the laser is switched back on. Both the transmission and the fluorescence recovered their initial levels, i.e. before any particle was trapped. Since the free moving particle did not travel far away from the trap while the trapping laser was off, the particle is trapped again briefly after switching the laser back on. The clear possibility to release the particle by simply switching off the trapping laser proves the particle was indeed trapped and not adsorbed.

Trapping vs. adsorption (fiber configuration under external illumination)

In a similar manner as in the case of a planar sample we checked that the particle was not adsorbed at the surface when using the fiber configuration under external illumination. For this particular configuration the fiber was fixed, the fluorescence was then collected through a microscope objective aligned in order to collect the fluorescence around the antenna. Figure SI2 presents the fluorescence of the bead and transmission through the antenna for the trapping of a 50 nm PS bead. At approximately t=30 s, both transmission and fluorescence show the trapping of a single particle. The particle was kept in the trap until t=270 s when the trapping laser was switched off. Shortly after (20 s), the trapping laser was switched back on. After this interruption of the trapping laser, the transmission and the fluorescence both reverted to their initial levels (before any particle was trapped), clearly proving the particle was not adsorbed to the surface.

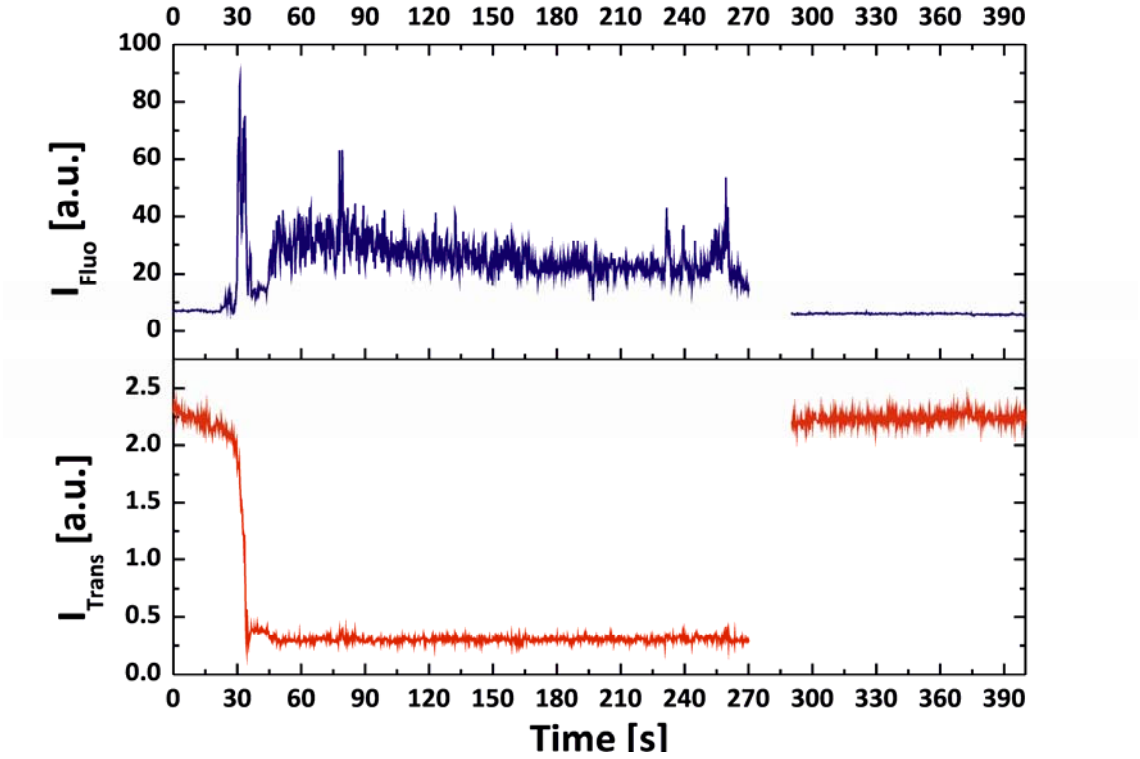

Figure SI2 : Experimental time trace showing trapping and release of a single 50 nm trapped particle: At t=270 s both the trapping laser and the green laser are switched off until t=290 s.

Trapping vs. adsorption (fiber configuration with illumination through the fiber)

For this configuration, no objectives where used to collect the signal in order to obtain a self contained system consisting of only the fiber to both trap and monitor trapping by the change of the reflected light coupling backwards in the fiber mode. Consequently, no fluorescence signal was collected. Yet, we could verify the particle was not adsorbed during the experiment by examining the reflection from the antenna. Figure SI3 presents the signal back reflected from the antenna during the trapping and release of a 50 nm PS bead. After an unstable trapping phase (40 s < t < 135 s), the particle is stably trapped for more than 60 s until the trapping laser was switched off at t=215 s. Soon after the trapping laser was switched back on, and the signal clearly restored back to its initial level showing the particle was not adsorbed. To overcome the high noise level, the histogram was fitted using two Gaussian distributions related to the different states of the system: no particle trapped and one particle trapped. This double fit (in red) shows a very good agreement with the data points, clearly demonstrating one particle was trapped for over a minute, then released by simply switching off the trapping laser during a short time.

DOI: 10.1038/NNANO.2014.24

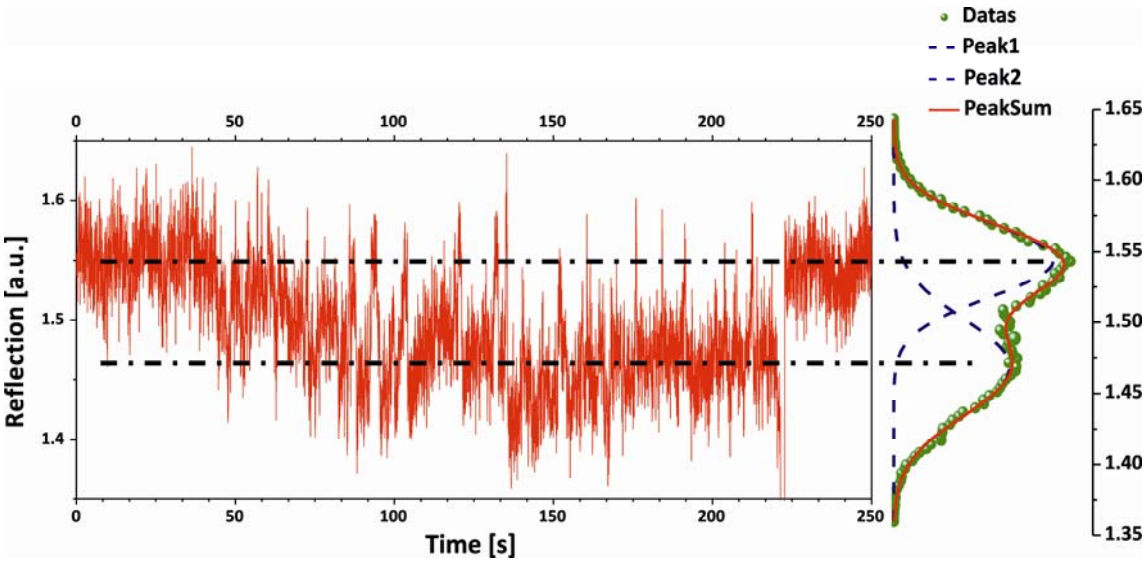

Figure SI3 : **Analysis of the time trace showing trapping of a 50 nm PS particle at the apex of the patterned fiber**: Histogram of the time trace (green dots). The dots are fitted with a sum of two Gaussian functions (red line). The centre of each Gaussian peak is located by a black dot-dashed line**.**

use of water as casting and/or developing solvent, or on eliminating environmentally harmful components from existing resists[7,8]. However, the idea of exploiting the solubility switching of silk is unique in the field of resists, and provides an approach that combines naturally inspired bottom-up self-assembly fabrication with the precision of a traditional top-down technique[9].

In addition to standard lithographic performance, Omenetto and colleagues also demonstrate the potential of silk fibroin as a functional resist material: that is, a resist that has specific properties useful for practical purposes other than surface patterning. For example, by doping the resist with quantum dots or with green fluorescent protein, the researchers prepare photonic crystal structures and observe clear fluorescence enhancement. Moreover, they show that the silk protein structures can protect encapsulated biological dopants, such as enzymes, from electron-beam irradiation and vacuum exposure. This property allows them to make a horseradish-based peroxidize sensor array in a single fabrication step (Fig. 1c).

A silk fibroin resist has the potential to benefit a wide range of bio-nano device applications. For such purposes, however, it is essential to reduce the required electron-beam dose, at least to levels commensurate with those used with typical electron-beam resists such as poly(methyl methacrylate). Nevertheless, by taking advantage of the polymorphic transformations of silk proteins to drive changes in solubility, Omenetto and colleagues have provided a stimulating new approach to the field of electron-beam lithography. ❐

Alex Robinson is at the School of Chemical Engineering, University of Birmingham, Edgbaston, Birmingham B15 2TT, UK.
e-mail: a.p.g.robinson@bham.ac.uk

References
1. Omenetto, F. G. & Kaplan, D. L. *Science* **329,** 528–531 (2010).
2. Kim, S. *et al. Nature Photon.* **6,** 818–823 (2012).
3. Mukherjee, C., Hota, M. K., Naskar, D., Kundu, S. C. & Maiti, C. K. *Phys. Status Solidi A* **210,** 1797–1805 (2013).
4. Bhumiratana, S. *et al. Biomaterials* **32,** 2812–2820 (2011).
5. Kim, S. *et al. Nature Nanotech.* **9,** 306–310 (2014).
6. Levinson, H. J. *Jpn. J. Appl. Phys.* **50,** 06GA01 (2011).
7. Satoshi Takei, S., Oshima, A., Wakabayashi, T., Kozawa, T. & Tagawa, S. *Appl. Phys. Lett.* **101,** 03106 (2012).
8. Sun, W. *et al. Arch. Environ. Contam. Toxicol.* **64,** 187–197 (2013).
9. Onses, S. M. *et al. Nature Nanotech.* **8,** 667–675 (2013).

Published online: 23 March 2014

OPTICAL TWEEZERS

Dressed for success

Controlled optical manipulation of a single dielectric nanoparticle is achieved with a bowtie nanoantenna placed at the end of the probe of a near-field scanning microscope.

Patrick C. Chaumet and Adel Rahmani

Since Arthur Ashkin demonstrated in 1970 that light can be used to trap particles[1], optical trapping has become a staple of atomic physics, optics and even biology. Optical tweezers, in particular, use focused laser beams to trap and manipulate small objects such as biological cells[2], bacteria and viruses[3]. Despite the success of optical trapping at the atomic (~0.1 nm) and microscopic (~1–10 μm) scales, trapping and manipulation of a single, dielectric nanoparticle (~50 nm) has been an elusive goal. Now writing in *Nature Nanotechnology*, Romain Quidant and co-workers from the Institut de Ciencies Fotoniques and Institució Catalana de Recerca i Estudis Avancats in Barcelona, and Macquarie University in Sydney report on the demonstration of optical trapping and three-dimensional manipulation of a single, 50-nm dielectric particle[4]. The researchers use optical forces to trap single particles, manipulate them over several micrometres, and release them without damaging them.

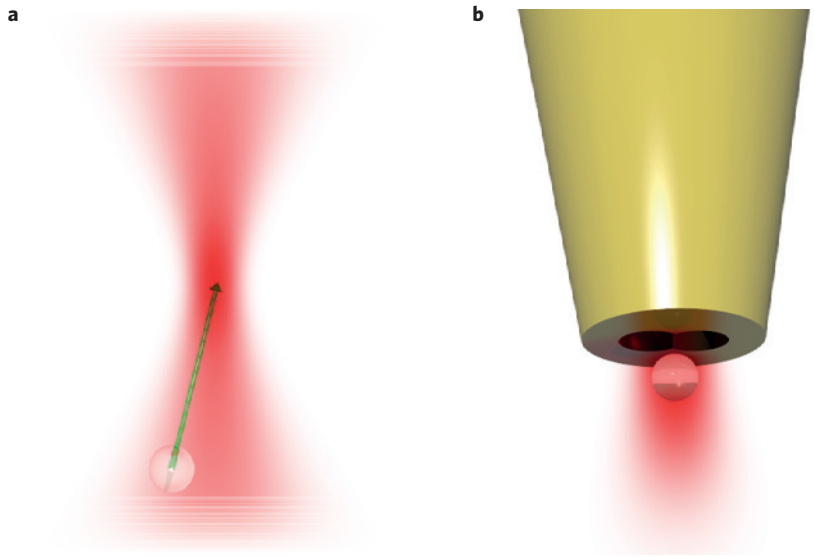

Figure 1 | Reducing the size of an optical trap. **a**, Schematic of a standard optical tweezer. When a particle is illuminated by a focused laser beam, the gradient force attracts the particle towards the higher-intensity area (green arrow). **b**, Near-field scanning optical microscope probe with a particle trapped at its apex.

To appreciate the ingenuity of the technique developed by Quidant and co-workers we can consider the case of a laser beam focused on a small, spherical, lossless, dielectric particle in a fluid (for example, water). We can separate the optical force into two contributions. The scattering force (radiation pressure), results from the light bouncing off the particle and scales as $(a/\lambda)^6$, where a is the particle radius and λ the wavelength of the laser beam. The gradient force is associated with spatial variations of the intensity of light, and scales as $(a/\lambda)^3$. For a nanoparticle $a < \lambda$, and thus, in general, the gradient force is the dominant contribution, attracting the particle towards

high-intensity regions (Fig. 1a). However, due to the small size of the nanoparticle the gradient force remains weak and Brownian motion within the fluid is constantly nudging it in random directions, thus hindering its trapping. As the optical force is proportional to the irradiance of light (intensity per unit of surface area), it could be possible to increase the power of the laser to overcome Brownian motion. However, a high irradiance could damage or even destroy the nanoparticle. Hence, the first challenge is to generate an optical trap for a moderate irradiance. A second, more subtle issue is that to trap a single nanoparticle the size of the trap should be of the order of the nanoparticle size. Such a small optical trap would be so sensitive to its environment that the interaction with the single nanoparticle that should be trapped may perturb it enough to destroy its trapping ability.

The technique presented by Quidant and co-workers overcomes these problems by using a modified near-field scanning optical microscope (NSOM) probe to create a subwavelength optical trap (Fig. 1b) and exploit, rather than fight, the trap's high sensitivity to its environment. The idea of using a NSOM probe for optical manipulation is not new[5,6]. The implementation of this idea, however, was hindered by the challenge of obtaining a strong enough trapping potential at a reasonable irradiance. The solution was to introduce a bowtie aperture at the end of the near-field probe (Fig. 2). Whereas, a NSOM probe usually consists of a chemically etched, metal-coated optical fibre with a round opening at the end, the authors' probe has a bowtie opening at its apex. The bowtie acts as a plasmonic nanoantenna, confining light on a subwavelength scale. The associated large gradient of the electric field

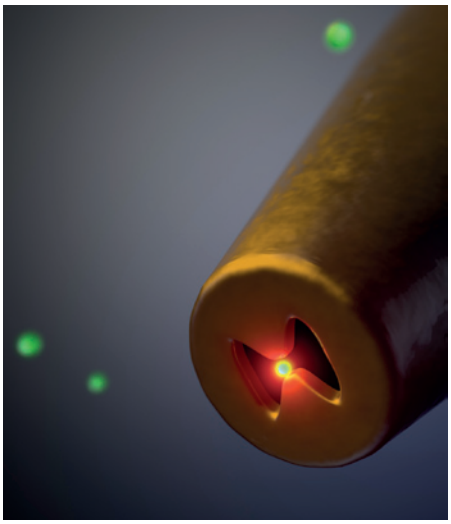

Figure 2 | Schematic of the optical nanotweezers. A nanoparticle is trapped near a bowtie plasmonic aperture at the end of a near-field optical probe. Image courtesy of Johann Berthelot.

ensures that, when light is funnelled down the probe, an efficient optical trap is created at the apex. To make sure that the sensitivity of such a trap could be used as an advantage, Quidant and co-workers modified the bowtie nanoantenna such that its resonance is slightly blue-shifted compared with the trapping wavelength. This way only when a nanoparticle is present near the bowtie opening is the optical trap activated. The result is an efficient optical trap for a relatively weak irradiance. Because the trap is formed at the tip of a NSOM probe, the trapped nanoparticle can be moved at will, and released by turning the illumination off.

The next challenge is to selectively trap a single nanoparticle. In the current scheme a particle has to wander near the bowtie to activate the optical trap, many applications would require an ability to locate a specific particle and capture it. If the nanoparticles are on a substrate, a bowtie nanoantenna probe can be a very effective, polarization-sensitive imaging device[7]. Local spectroscopy via the probe could provide a way to discriminate between different types of nanoparticle. This would be particularly interesting with metallic nanoparticles. The nanoantenna at the end of the NSOM probe could be tailored to a particular plasmon resonance for material-selective, or even size-selective trapping. We can also envisage an array of near-field probes[8] to capture and manipulate particles attached to different antigen–antibody complexes or DNA strands. As a result of the nanoantennas being at the apices of the probes, a nanoscale immunoassay or DNA biochip based on the selective capture and the parallel detection of biomolecules could be possible. ❐

Patrick C. Chaumet is at Aix Marseille Université, CNRS, Centrale Marseille, Institut Fresnel, UMR 7249, 13013 Marseille, France. Adel Rahmani is at the School of Mathematical Sciences, University of Technology Sydney, Broadway, New South Wales 2007, Australia.
e-mail: patrick.chaumet@fresnel.fr; Adel.Rahmani@uts.edu.au

References

1. Ashkin, A. *Phys. Rev. Lett.* **24,** 156–159 (1970).
2. Ashkin, A., Dziedzic, J. M. & Yamane, T. *Nature* **330,** 769–771 (1987).
3. Ashkin, A. & Dziedzic, J. M. *Science* **235,** 1517–1520 (1987).
4. Berthelot, J. *et al. Nature Nanotech.* **9,** 295–299 (2014).
5. Novotny, L., Bian, R. X. & Xie, X. S. *Phys. Rev. Lett.* **79,** 645–648 (1997).
6. Chaumet, P. C., Rahmani, A. & Nieto-Vesperinas, M. *Phys. Rev. Lett.* **88,** 123601 (2002).
7. Vo, T.-P. *et al. Opt. Express* **20,** 4124–4135 (2012).
8. Chovin, A., Garrigue, P., Manek-Honninger, I. & Sojic, N. *Nano Lett.* **4,** 1965–1968 (2004).

NANOSCALE MRI

Dark spins in the spotlight

A single nitrogen–vacancy centre can be used to probe the location of electron spins with subnanometre precision.

Lloyd Hollenberg

The material and quantum properties of the negatively charged nitrogen–vacancy (NV) centre in diamond provide a range of quantum technology possibilities, including nanoscale sensing and imaging[1,2]. Remarkably, the electronic spin states of NV centres have relatively long quantum coherence at room temperature, making them a sensitive probe for a variety of external perturbations. The NV centre can be tracked and read-out optically; its position, local magnetic and electric fields, and temperature can all be monitored through quantum control via the application of microwaves. Furthermore, these properties lend themselves to biosensing applications as diamond is relatively bio-friendly[3–7]. A number of papers have reported the use of NVs as sensors of electronic and nuclear spins in nanoscale volumes[8–13], including in biological contexts[14–16]. Writing in *Nature Nanotechnology*, Mike Grinolds and co-workers from Harvard University,